


T2*-based MR imaging (gradient echo or susceptibility-weighted imaging) in midline and off-midline intracranial germ cell tumors: a pilot study

Giovanni Morana¹  · Cesar Augusto Alves² · Domenico Tortora¹ · Jonathan L. Finlay³ · Mariasavina Severino¹ · Paolo Nozza⁴ · Marcello Ravegnani⁵ · Marco Pavanello⁵ · Claudia Milanaccio⁶ · Mohamad Maghnie⁷ · Andrea Rossi¹ · Maria Luisa Garrè⁶

Received: 14 August 2017 / Accepted: 6 November 2017 / Published online: 11 November 2017
© Springer-Verlag GmbH Germany, part of Springer Nature 2017

Abstract

Purpose The role of T2*-based MR imaging in intracranial germ cell tumors (GCTs) has not been fully elucidated. The aim of this study was to evaluate the susceptibility-weighted imaging (SWI) or T2* gradient echo (GRE) features of germinomas and non-germinomatous germ cell tumors (NGGCTs) in midline and off-midline locations.

Methods We retrospectively evaluated all consecutive pediatric patients referred to our institution between 2005 and 2016, for newly diagnosed, treatment-naïve intracranial GCT, who underwent MRI, including T2*-based MR imaging (T2* GRE sequences or SWI). Standard pre- and post-contrast T1- and T2-weighted imaging characteristics along with T2*-based

MR imaging features of all lesions were evaluated. Diagnosis was performed in accordance with the SIOP CNS GCT protocol criteria.

Results Twenty-four subjects met the inclusion criteria (17 males and 7 females). There were 17 patients with germinomas, including 5 basal ganglia primaries, and 7 patients with secreting NGGCT.

All off-midline germinomas presented with SWI or GRE hypointensity; among midline GCT, all NGGCTs showed SWI or GRE hypointensity whereas all but one pure germinoma were isointense or hyperintense to normal parenchyma. A significant difference emerged on T2*-based MR imaging among midline germinomas, NGGCTs, and off-midline germinomas ($p < 0.001$).

Conclusion Assessment of the SWI or GRE characteristics of intracranial GCT may potentially assist in differentiating pure germinomas from NGGCT and in the characterization of basal ganglia involvement. T2*-based MR imaging is recommended in case of suspected intracranial GCT.

GM and CAA are joint first authors and contributed equally to this study.

AR and MLG are joint last authors and contributed equally to this study.

Electronic supplementary material The online version of this article (<https://doi.org/10.1007/s00234-017-1947-3>) contains supplementary material, which is available to authorized users.

✉ Giovanni Morana
giovannimorana@gaslini.org

- ¹ Neuroradiology Unit, Istituto Giannina Gaslini, Genoa, Italy
- ² Radiology Department, Hospital Das Clinicas, Sao Paulo, Brazil
- ³ Division of Hematology, Oncology and BMT, Nationwide Children's Hospital and The Ohio State University, Columbus, OH, USA
- ⁴ Pathology Unit, Istituto Giannina Gaslini, Genoa, Italy
- ⁵ Neurosurgery Unit, Istituto Giannina Gaslini, Genoa, Italy
- ⁶ Neuro-oncology Unit, Istituto Giannina Gaslini, Genoa, Italy
- ⁷ Pediatric Endocrine Unit, Istituto Giannina Gaslini, University of Genoa, Genoa, Italy

Keywords SWI · Germinoma · Germ cell tumors · NGGCT · Gradient echo · Brain tumor

Introduction

Intracranial germ cell tumors (GCTs) are rare and heterogeneous neoplasms with variable geographic incidence, accounting for approximately 2–3% of pediatric brain tumors in Western countries and 10% in Far East Asian countries [1–3].

GCT peak incidence is during adolescence, and approximately 90% occur before age 20 years [4].

Based on the histologic components, response to treatment, and prognosis, GCTs are classically categorized into germinomas

and non-germinomatous germ cell tumors (NGGCTs), with pure teratomas (mature and/or immature) often considered a separate category [5].

Intracranial GCTs arise predominantly in midline supratentorial locations, such as the suprasellar and pineal regions; however, about 6–10% of these neoplasms arise in off-midline intracranial structures, usually comprising the basal ganglia and thalamus [6, 7], and much more rarely the cerebellum [8, 9]. Pure germinomas have generally a good prognosis with 5-year overall survival (OS) rates >90%, whereas high relapse risk and poor outcome are associated with NGGCT (5-year OS rates of 30–50%) [5].

Histological confirmation represents the gold standard for accurate tumor characterization; however, current consensus on the management of intracranial GCT in North America and Europe maintains that patients with consistent radiological imaging and α -fetoprotein (AFP) and/or beta-human chorionic gonadotropin (BHCG) elevations in the serum and/or cerebrospinal fluid (CSF) above defined thresholds do not require surgical biopsy, so that treatment may be initiated based on the diagnosis suggested by the marker elevation and neuroimaging [10, 11].

Conventional magnetic resonance imaging (MRI), including T1-, T2-, and gadolinium-enhanced T1-weighted sequences, is the current radiological standard to evaluate intracranial GCT [12]. Nevertheless, even though certain imaging characteristics may be helpful to suggest a diagnosis, differentiating pure germinomas from NGGCT is not straightforward by standard neuroimaging alone due to overlapping features. At the same time, GCT arising in atypical locations may present with ambiguous and non-specific conventional imaging findings, often causing delayed recognition.

T2*-based MR imaging, including conventional T2* gradient echo (GRE) sequences or susceptibility-weighted imaging (SWI), may be very helpful in depicting hemorrhagic components (especially microbleeds), calcifications, or biologic metal accumulation in lesions and tissues [13].

Clinical applications of T2*-based MR imaging in children are extremely wide including, but not limited to, head trauma, stroke, epilepsy, vascular malformations, and brain tumors [13, 14].

In the setting of GCT, few data are available [8, 15, 16]. On the basis of these considerations, the overall objective of this retrospective study was to analyze the SWI or T2* GRE features of midline and off-midline GCT. Specifically, we aimed to test the ability of T2*-based MR imaging in discriminating pure germinomas from NGGCT.

Methods

Subjects

We retrospectively evaluated all consecutive pediatric patients (aged less than 18 years at diagnosis) referred to our institution

between 2005 and 2016 for newly diagnosed, treatment-naïve intracranial GCT, who underwent MRI, including T2*-based MR imaging (T2* GRE sequences or SWI).

Information regarding sex, age at diagnosis, clinical presentation, CSF cytology and serum and/or CSF AFP and BHCG levels was noted.

In accordance with the SIOP CNS GCT 96 and SIOP CNS GCT II protocols, all patients with serum AFP >25 ng/ml or BHCG >50 IU/l or CSF AFP >25 ng/ml or CSF BHCG >50 IU/l were diagnosed as NGGCT and biopsy was avoided. Patients with serum and CSF markers below these thresholds received histological confirmation, except for cases of imaging-confirmed bifocal (suprasellar and pineal) tumors which were considered pure germinomas.

This study was conducted within the guidelines from our institutional review board, and informed consent was obtained in all cases.

Image protocol and analysis

All MRI studies were performed on a 1.5-T superconductive system (Intera Achieva; Philips, Best, the Netherlands) using an 8-channel parallel imaging head coil; these studies included 3-mm-thick sagittal spin echo (SE) T1- and turbo spin echo (TSE) T2-weighted images; 4-mm-thick axial fluid attenuation inversion recovery (FLAIR), SE T1-, and TSE T2-weighted images; and 4-mm-thick coronal TSE T2-weighted images. Imaging parameters were as follows: TR 805 ms, TE 12 ms, and NEX 2, for SE T1 weighting; TR 5580 ms, TE 100 ms, and NEX 2, for TSE T2 weighting; and TR 11,000 ms, TE 140 ms, TI 2800 ms, and NEX 2, for FLAIR. Following gadolinium compound bolus administration (0.1 mmol/kg, macrocyclic ionic agent), 4-mm-thick axial and coronal and 3-mm-thick sagittal SE T1-weighted images were acquired in all patients. A post-contrast axial 3D T1-weighted fast field echo (FFE) sequence with the following parameters, TR 14 ms, TE 3.9 ms, flip angle 25°, and NEX 1, was acquired in addition to post-contrast SE sequences in 17 subjects.

T2*-based MR imaging included either conventional T2* GRE sequences with the following parameters (TR 759 ms, TE 23 ms, flip angle 18°, NEX 2) or SWI, performed before contrast agent administration. The SWI sequence was a 3D, fully flow-compensated fast field echo sequence with the following parameters: TR 57 ms, TE 40 ms, 96 sections, flip angle 15°.

SWI was available in 10 patients, whereas T2* GRE in 14. None were examined with both techniques.

Computed tomography (CT), available in 15 patients, was included in the analysis.

All images were assessed in consensus by two neuroradiologists (GM and CAA), focusing on CT and conventional MRI characteristics (tumor location, T1- and T2-weighted

signal intensity, presence of cysts, calcifications, perifocal edema, and contrast enhancement pattern). T2*-based MR imaging features were also evaluated (signal intensity with respect to normal parenchyma and compared to CT, T1- and T2-weighted imaging).

Statistical analysis was performed by using SPSS Statistics for Mac, version 21.0 (IBM, Armonk, NY). A *p* value of 0.05 was used to define nominal statistical significance.

Chi-squared test was performed to assess differences on T2* GRE/SWI, conventional pre-contrast T1-/T2-weighted images, or contrast-enhanced images among midline and off-midline GCT.

Results

Clinical features

A total of 24 subjects met the inclusion criteria. In the series, there were 17 males and 7 females. Age at diagnosis ranged from 8 to 17 years (median, 13 years). Eleven lesions were located in the pineal region (46%), 4 were along the hypothalamic-pituitary axis (17%), 4 were bifocal (17%), 2 presented with isolated involvement of the basal ganglia (8%), and 3 showed concomitant involvement of the hypothalamic-pituitary axis and basal ganglia (12%).

Seven patients presented with increased serum or CSF tumor markers and, according to SIOP CNS GCT criteria, biopsy was avoided and they were classified as NGGCT (3 pineal, 1 sellar-suprasellar, 3 bifocal). Biopsy was also avoided in a patient with synchronous involvement of the pineal and suprasellar region and negative tumor markers, indicative of a pure germinoma. In the remaining 16 patients, the diagnosis of pure germinoma (8 pineal, 3 sellar-suprasellar, 2 isolated basal ganglia, and 3 with concomitant suprasellar and basal ganglia involvement) was established histopathologically by biopsy or open surgery.

Main clinical findings are summarized in Table 1.

Neuroimaging

On SWI or T2* GRE imaging, all NGGCTs (7/7, 100%) demonstrated prominent hypointense foci in the parenchymal portion of the lesion, compatible with iron/blood products (Fig. 1a–h).

On conventional imaging, two out of seven NGGCTs (29%) presented with homogeneous signal on T1- and/or T2-weighted imaging whereas the remaining five lesions (71%) were heterogeneous, including foci of spontaneous T1 hypersignal and cystic components (ranging in size between 0.5 and 1 cm).

All but one pure germinoma involving midline structures (14/15, 93%) showed on SWI/T2* GRE an isointense or

Table 1 Summary of subject characteristics

No. of subjects	24	
Sex		
Male	17 (71%)	
Female	7 (29%)	
Age at diagnosis		
Median	13	
Range	8–17	
Diagnosis according to SIOP criteria		
Germinoma	17	
NGGCT	7	
Tumor locations		
Germinoma	IS-SS	3
	Pineal	8
	Bifocal	1
	Isolated BG	2
	IS-SS and BG	3
NGGCT	IS-SS	1 ^a
	Pineal	3
	Bifocal	3
Main clinical presentation		
Germinoma	IS-SS	DI, VD
	Pineal	IICP
	Bifocal	DI
	BG	DI/LW/HP
NGGCT	IS-SS	DI/MPHD
	Pineal	IICP, PS
	Bifocal	DI
Disease stage		
Germinoma	Localized	14
	Metastatic	3
NGGCT	Localized	6 ^b
	Metastatic	1

NGGCT non-germinomatous germ cell tumor, IS intrasellar, SS suprasellar, BG basal ganglia, DI diabetes insipidus, VD visual disturbances, IICP increased intracranial pressure, LW limb weakness, HP hemiparesis, MPHD multiple pituitary hormone deficits, PS Parinaud syndrome

^a Subject with concomitant suspected basal ganglia involvement only on SWI (Fig. 4)

^b One subject with suspected cerebellar dissemination only on SWI (Fig. 3)

slightly hyperintense signal of the parenchymal portion of the lesion when compared to normal brain (Fig. 1i–p). In one subject with a huge sellar-suprasellar germinoma extending to both cavernous sinuses, scattered tiny hypointense foci on SWI were present whereas the bulk of the lesion appeared isointense. On conventional imaging, 6 out of 15 (40%) midline germinomas presented a heterogeneous signal on T1- and/or T2-weighted imaging, including tiny cystic components (smaller than 0.5 cm in almost all cases). Perifocal edema

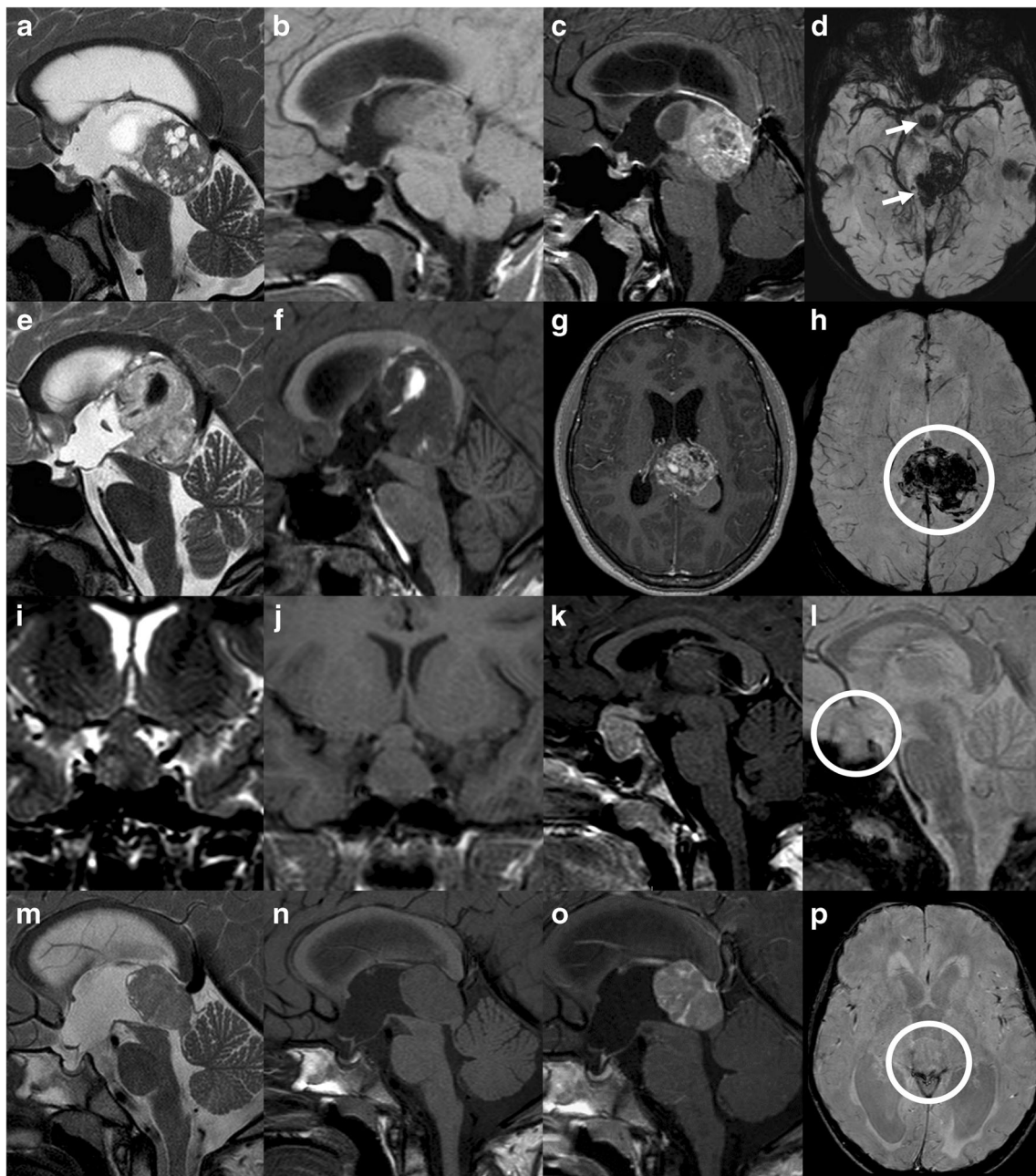


Fig. 1 MRI features of NGGCTs and germinomas. **a–d** Bifocal NGGCT in a 13-year-old boy. Sagittal T2- (**a**), T1- (**b**), and gadolinium-enhanced T1-weighted (**c**) images reveal a heterogenous solid cystic mass lesion in the pineal region. The posterior pituitary bright spot is absent (**b**). There is concomitant pathologic thickening of the infundibular recess of the third ventricle. Axial SWI image shows marked hypointensity of both the pineal and the suprasellar lesions (arrows, **d**). **e–h** Pineal NGGCT in a 17-year-old boy. Sagittal T2- (**e**) and T1-weighted (**f**) images reveal a huge pineal mass lesion with a central hemorrhagic area, hypointense on T2- and spontaneously hyperintense on T1-weighted images. Axial post-contrast T1-weighted image (**g**) shows heterogeneous enhancement.

SWI demonstrates marked hypointensity of the whole lesion (circle, **h**). **i–l** Sellar-suprasellar germinoma in a 13-year-old girl. Coronal T2- (**i**), T1- (**j**), and sagittal gadolinium-enhanced T1-weighted (**k**) images demonstrate a sellar-suprasellar mass lesion with homogeneous signal both pre- and post-contrast. On sagittal T2* GRE image, the lesion shows a homogeneous isointense signal (circle, **l**). **m–p** Pineal germinoma in a 12-year-old boy. Sagittal T2- (**m**) and T1-weighted (**n**) images show a pineal mass lesion. There are few tiny cysts along the ventral pole of the lesion (**m**); following gadolinium administration, there is slight heterogeneous enhancement. Axial SWI image demonstrates isointense signal (circle, **p**)

was found in three cases (20%) (all lesions involving the pineal region with thalamic edema). Following gadolinium administration, homogeneous, moderate to marked

enhancement was present in seven cases (47%), whereas there was heterogeneous enhancement in eight (53%).

The presence of SWI or T2* GRE hypointensity was identified in all off-midline pure germinomas.

Germinomas with basal ganglia involvement presented with heterogeneous signal on T1- and/or T2-weighted imaging in four out of five subjects (80%). Following gadolinium administration, heterogeneous enhancement was present in two cases, whereas three did not show contrast enhancement.

A significant difference was demonstrated on T2*-based MR imaging among midline germinomas, NGGCTs, and off-midline germinomas ($p < 0.001$). No significant differences emerged on conventional pre- ($p = 0.183$) and post-contrast imaging ($p = 0.372$) among the three groups. Main neuroimaging findings in midline and off-midline GCT are summarized in Table 2.

In midline GCT, calcifications were detected only in the pineal region, both in pure germinomas and in NGGCTs. Among germinomas involving the basal ganglia, CT was available in one subject, without evidence of calcifications.

Three out of five patients with basal ganglia involvement presented with unilateral atrophy of the cerebral hemisphere and/or cerebral peduncle.

Of note, in a patient with suprasellar involvement and concomitant left basal ganglia abnormalities characterized by a small cystic lesion and non-specific T2/FLAIR hyperintensity without contrast enhancement, SWI revealed marked hypointensity of the left globus pallidus, suggestive of concomitant left basal ganglia involvement. Following chemotherapy and radiotherapy, these abnormalities reduced on follow-up on conventional imaging in keeping with a pattern of concomitant midline and off-midline involvement; SWI also revealed reduced hypointensity. In the same patient, there was also marked SWI hypointensity of the right globus pallidus, suspicious for additional involvement. On conventional imaging, there was only a small, focal, and non-specific T2/FLAIR hyperintensity at that level. On follow-up, the SWI hypointensity persisted whereas the T2/FLAIR hyperintensity was no longer visible (Fig. 2).

T2*-based MR imaging was available on follow-up in three additional patients with pure germinomas involving the

basal ganglia, demonstrating persistent hypointensity in one subject and reduction in two.

In a patient with sellar-suprasellar NGGCT and marked SWI hypointensity of the whole lesion, SWI revealed additional hypointense foci along the cerebellar folia, without corresponding abnormalities on standard pre- and post-contrast MRI. These lesions were considered suspicious for secondary dissemination and demonstrated reduction following treatment (Fig. 3).

In a patient with bifocal and disseminated NGGCT, SWI demonstrated bilateral basal ganglia hypointensity, without corresponding abnormalities on T1-/T2-weighted imaging; foci of dissemination were also hypointense on SWI (Fig. 4). In the same patient, SWI was performed at recurrence and following re-treatment, demonstrating progressive accumulation of hypointense foci along the margins of the ventricular system, later corresponding to foci of dissemination on post-contrast imaging (Fig. 5 and supplementary Figure S1).

Three out of 15 patients with pure germinomas involving midline structures were metastatic at presentation on conventional imaging; in these patients, T2*-based MR imaging did not reveal hypointense lesions.

Discussion

The role of T2*-based MR imaging in intracranial GCT has not been fully investigated. In our study, T2*-based MR imaging revealed significant differences among midline and off-midline germinomas and NGGCTs.

Prior studies evaluating large series of intracranial GCT have demonstrated that conventional MRI is very sensitive in detecting suprasellar and pineal region masses, but the radiographic characteristics may be similar among GCT, therefore limiting their usefulness in determining their exact histology [5]. Several imaging features have been analyzed including calcifications, presence of cysts, and pattern of contrast

Table 2 Summary of MRI findings of midline NGGCTs, germinomas, and basal ganglia germinomas

	MRI signal	Midline NGGCTs	Midline germinomas ^a	Basal ganglia germinomas ^a	<i>p</i> value ^b
T1/T2	Homogeneous	2/7	9/15	1/5	$p = 0.183$
	Heterogeneous ^c	5/7	6/15	4/5	
T1 CE	Homogeneous	2/7	7/15	0 ^d	$p = 0.372$
	Heterogeneous	5/7	8/15	2/5	
GRE/SWI	Hypointense	7/7	1/15	5/5	$p < 0.001$
	Iso/hyperintense	0/7	14/15	0	

^a Three subjects with concomitant suprasellar and basal ganglia involvement. Each location was counted separately (27 locations in 24 subjects)

^b Value for chi-squared test (differences on T2* GRE/SWI, conventional pre-contrast T1-/T2-weighted images or contrast-enhanced images among midline NGGCTs, germinomas, and off-midline germinomas)

^c Including cystic components

^d No contrast enhancement

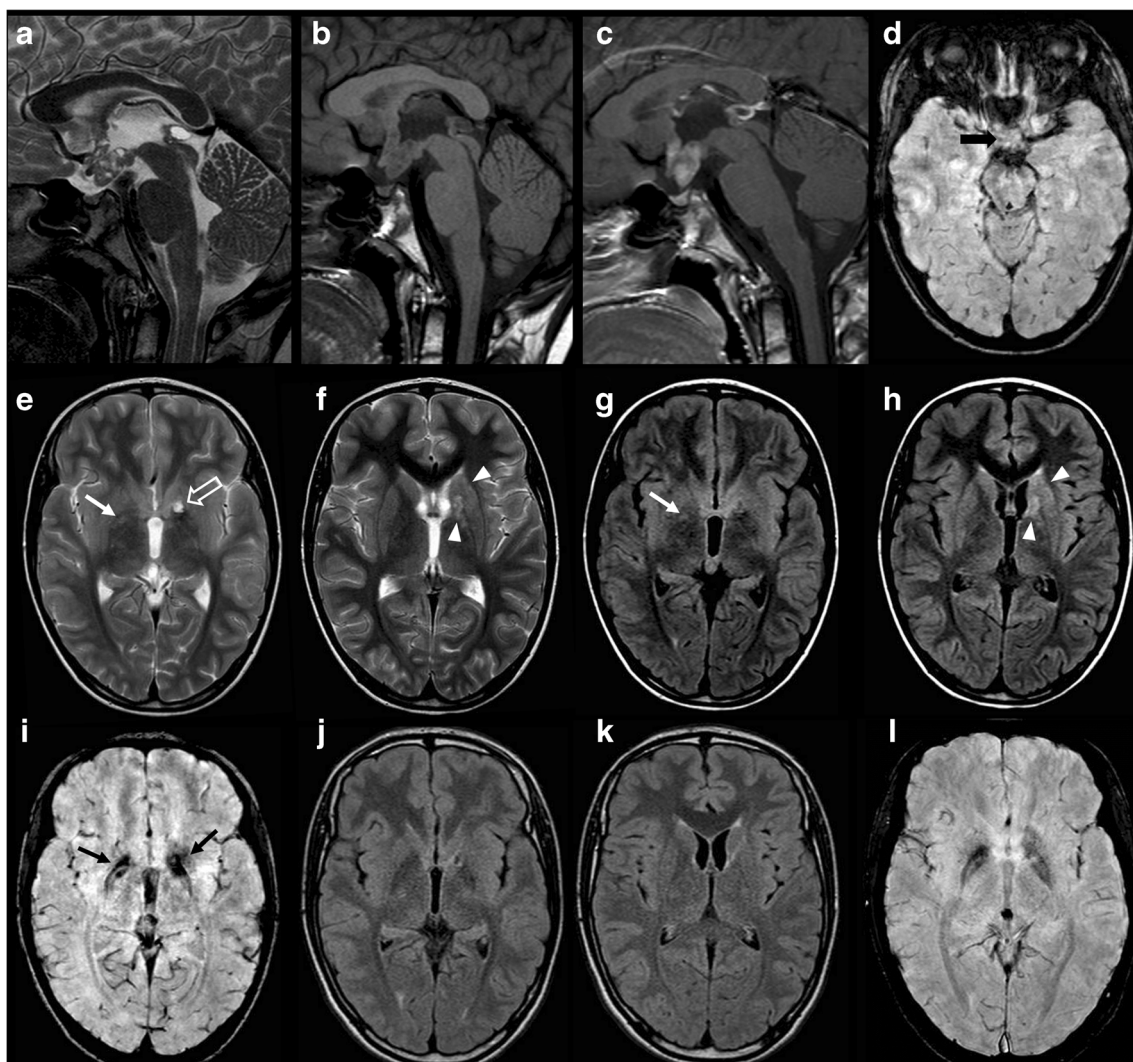


Fig. 2 Germinoma with synchronous involvement of midline and off-midline structures in a 9-year-old boy. Sagittal T2- (a), T1- (b), and gadolinium-enhanced T1-weighted (c) images show a suprasellar mass with multiple cystic components and heterogeneous contrast enhancement. The posterior pituitary bright spot is absent (b). There is an incidental pineal gland cyst. Axial SWI image shows isointense signal of the suprasellar mass (thick black arrow, d). Axial T2-weighted images (e, f) show a small cystic lesion (0.7 cm) with a dark fluid level in the left globus pallidus (open arrow, e) and irregular hyperintensity extending to the anterior limb of the internal capsule (arrowheads, f). A non-specific mild hyperintensity is also visible in the right globus pallidus (thin white arrow, e). Axial FLAIR images confirm a minimal hyperintensity in the

right globus pallidus (thin white arrow, g) and the left nucleo-capsular region abnormality (arrowheads, h). Pre- and post-contrast T1-weighted images (not shown) did not reveal definite abnormalities with the exception of a small focal hypointensity corresponding to the left basal ganglia cyst. Axial SWI image shows marked hypointensity in the left globus pallidus around and within the small cyst; there is also hypointensity involving the right globus pallidus (thin black arrows, i). On follow-up MRI (6 months after treatment), FLAIR images show marked reduction in size of the left basal ganglia hyperintensity and disappearance of the small right basal ganglia abnormality (j, k). SWI image (l), performed 6 years later, shows clear reduction of the left basal ganglia hypointensity and persistence on the right side

enhancement as possible findings to differentiate pure germinomas from NGGCT [17–20]. Additionally, the presence of spontaneous T1 hypersignal within the tumor, described as an indirect finding of hemorrhage, has already been evaluated, however without statistical difference between both subgroups [21]. In general, the standard neuroimaging characteristics of pure germinomas and NGGCTs are similar enough to limit diagnostic certainty, and either tissue confirmation or the measurement of specific tumor markers is needed for the diagnosis [22].

In our series, T1- and T2-weighted imaging features of GCT were in line with those of prior studies. On the contrary, T2*-based MR imaging demonstrated an isointense or slightly hyperintense signal in all but one pure midline germinoma (with the exception of calcifications) and prominent hypointense foci in all NGGCT extending beyond calcifications, in keeping with hemoglobin degradation products or iron accumulation. These findings suggest that T2*-based MR imaging might help in differentiating pure midline germinomas from NGGCT, even though larger series are

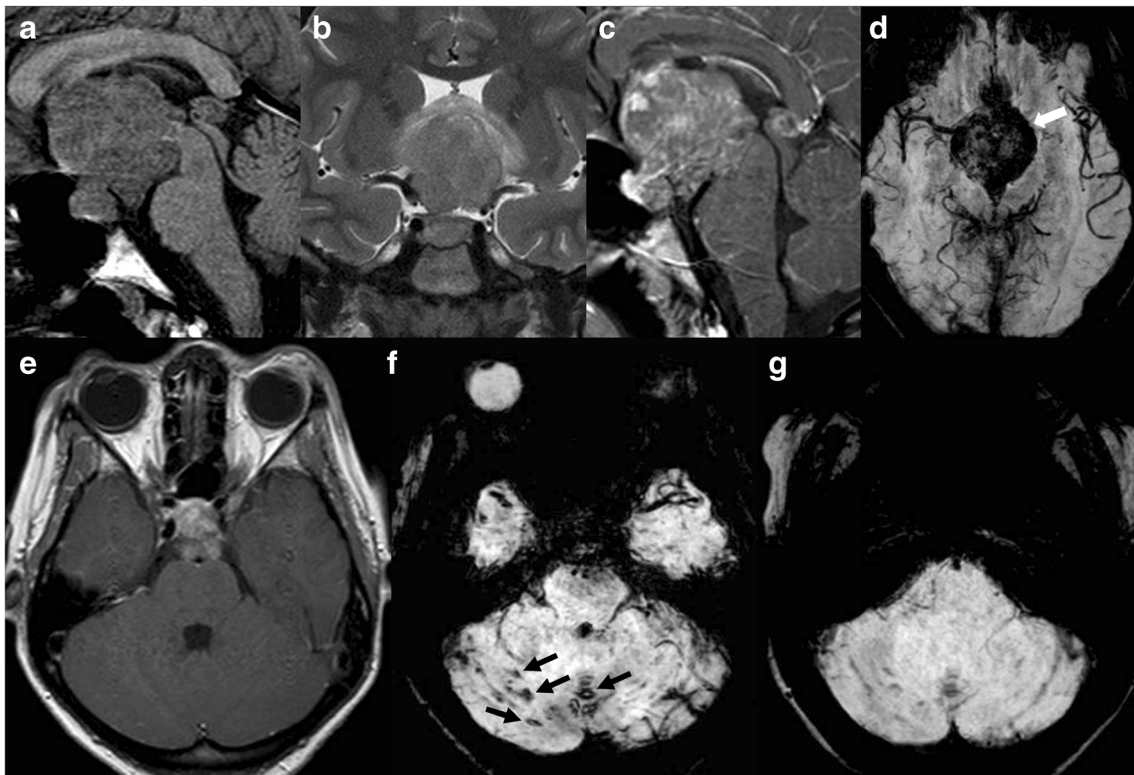


Fig. 3 Sellar-suprasellar NGGCT in a 17-year-old girl. Sagittal T1- (a) and coronal T2-weighted (b) images show a huge sellar-suprasellar mass lesion with homogeneous signal. The posterior pituitary bright spot is absent (a). Post-contrast sagittal T1-weighted image (c) shows heterogeneous enhancement. Axial SWI image demonstrates marked hypointensity of the whole lesion (thick white arrow, d), in keeping with extensive microbleeds not discernible from standard T1- and T2-weighted imaging. Gadolinium-enhanced axial T1-weighted image (e)

does not reveal areas of pathologic contrast enhancement along the cerebellum, whereas axial SWI image shows hypointense foci along the right cerebellar folia and vermis (thin black arrows, f), suspicious for microhemorrhagic secondary lesions. SWI performed 6 months after the end of treatment shows marked reduction of the cerebellar hypointense foci (g). At admission, there was no evidence of dissemination based on cerebrospinal fluid cytology; spinal MRI (not shown) was also negative

required to confirm these data. Regarding the role of T2*-based MR imaging in GCT, only small case descriptions are available in the literature. In a prior case series including six pediatric patients, Lou et al. [15] highlighted the potential role of SWI in the early recognition of basal ganglia germinoma. In that study, SWI clearly demonstrated the presence of basal ganglia hypointensity when only subtle and inconspicuous changes were depicted by conventional MRI.

In an additional case report, Minami et al. [8] underscored the diagnostic value of T2*-based MR imaging in an adult patient with intracranial GCT arising in the cerebellum and brain stem, presenting only with low-intensity spots on T2* GRE and SWI in the early phase of disease and with further evidence of contrast enhancement after 8 months; the authors concluded that enlarging low-intensity lesions on T2* GRE and SWI may be a reliable clue to the diagnosis of germinomas, irrespective of their location, even without enhancement.

In line with the findings reported by Lou et al. [15], basal ganglia involvement in pure germinomas was always characterized by the presence of hypointense foci. This confirms a different imaging behavior of midline and off-midline pure

germinomas. Interestingly, basal ganglia involvement was subtle and non-specific on standard MRI in two out of five cases with pure germinomas, whereas in one subject with NGGCT and disseminated disease, bilateral basal ganglia hypointensity raised the suspicion of additional involvement.

The pathogenesis underlying the low signal intensity on SWI in basal ganglia germinoma may be explained by the presence of blood products. Indeed, the majority of basal ganglia germinomas are characterized by the presence of hemorrhagic foci [17]. In addition to intratumoral hemorrhage, the SWI/GRE hypointensity of basal ganglia might be explained by tumor-induced iron accumulation, especially when hypointensity involves the globus pallidus. This structure is physiologically rich in biological metals, including iron and manganese. It has been hypothesized that axonal transport of transferrin may be disrupted by tumor invasion, resulting in iron deposition. Another hypothesis involves the possible tumor cell secretion of transferrin that binds to transferrin receptors on neurons and glial cells, thus promoting the transport of iron to the globus pallidus [15, 16, 23].

Regarding NGGCTs, they commonly may have associated hemorrhage, causing a more heterogeneous pattern of signal

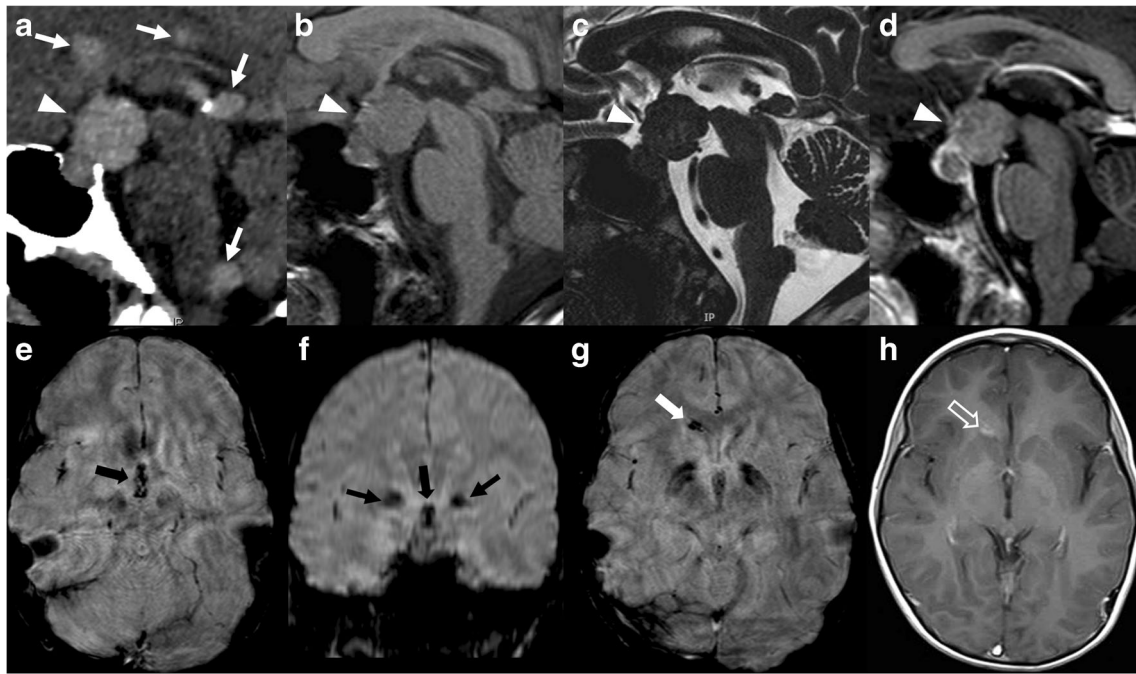


Fig. 4 Metastatic NGGCT in a 9-year-old girl. Sagittal CT image (a), T1- (b), T2- (c), and gadolinium-enhanced T1-weighted (d) images show a solid mass of the hypothalamic-hypophyseal region (arrowheads, a–d), demonstrating a compact and homogeneous structure. Concomitant pineal involvement and secondary lesions, better visible on the sagittal CT image (thin white arrows, a), demonstrate similar density of the primitive lesion (mild spontaneous hyperdensity). All lesions show weak contrast enhancement (d). Axial and coronal SWI images (e–g) demonstrate hypointense foci within the suprasellar lesion (thick black

arrow, e, f) and reveal marked hypointensity of the bilateral globus pallidus, without evidence of definite abnormalities on T2-weighted (not shown) and axial post-contrast T1-weighted image (h). On axial gadolinium-enhanced T1-weighted image, there is also mild enhancement of a secondary lesion located along the margin of the right frontal horn (open arrow, h), with corresponding hypointensity on SWI image (thick white arrow, g). Cytologic examination of cerebrospinal fluid was also positive for disseminated disease, whereas spinal MRI (not shown) was negative

intensity [5]. Intratumoral hemorrhage is particularly characteristic of choriocarcinoma and of mixed neoplasms with choriocarcinomatous elements, typically due to the fragility of its vessels [24].

In our series, calcifications of the pineal region appeared hypointense on SWI magnitude images and T2* GRE. When compared to conventional T2* GRE sequences, SWI offers the opportunity to discriminate iron and calcium on the basis of their paramagnetic-versus-diamagnetic behaviors using filtered phase images, thus reducing the need for additional CT [13, 14].

Bifocal tumors were both germinomas and secreting NGGCTs, whereas concomitant involvement of midline (suprasellar) and basal ganglia was found almost exclusively in pure germinomas. Review of the literature demonstrated that three additional cases of concomitant involvement of the suprasellar compartment and basal ganglia turned out to be all pure germinomas [9, 25, 26]. These findings suggest that this association is predictive of a GCT, facilitating an early recognition. In this context, the contribution of T2*-based MR imaging may be significant given the high sensitivity of this technique in the detection of basal ganglia involvement. This is especially true in case of a clinical presentation with diabetes insipidus, lack of the posterior pituitary bright spot, and

absence of a definite pituitary stalk thickening or hypothalamic mass lesion. In such cases, the search for basal ganglia abnormalities is strongly advised and may potentially reduce the diagnostic delay that typically characterizes these lesions. Of note, even though synchronous involvement of midline and off-midline structures is mainly found in pure germinomas, basal ganglia involvement in NGGCT can occur [24, 27, 28], demonstrating similar features to pure germinomas, therefore warranting histological verification.

Basal ganglia hypointensity on T2*-based MR imaging is rather uncommon in children. This MR finding indicates iron, calcium, or blood product deposition. Bilateral hypointensity is mainly found in genetic conditions (e.g., idiopathic basal ganglia calcification), congenital infections, hypoxic-ischemic encephalopathy (status marmoratus), metabolic/degenerative disorders (e.g., Wilson disease, neurodegeneration with brain iron accumulation, Cockayne syndrome, or mitochondrial disorders), or as a late consequence of radiotherapy (mineralizing microangiopathy) [29]. Bilateral basal ganglia germinoma may rarely occur and, in the appropriate clinical setting, bilateral basal ganglia hypointensity should raise the suspect of a germinoma [30].

An additional information offered by SWI at presentation was the detection of foci of hypointensity distant from the

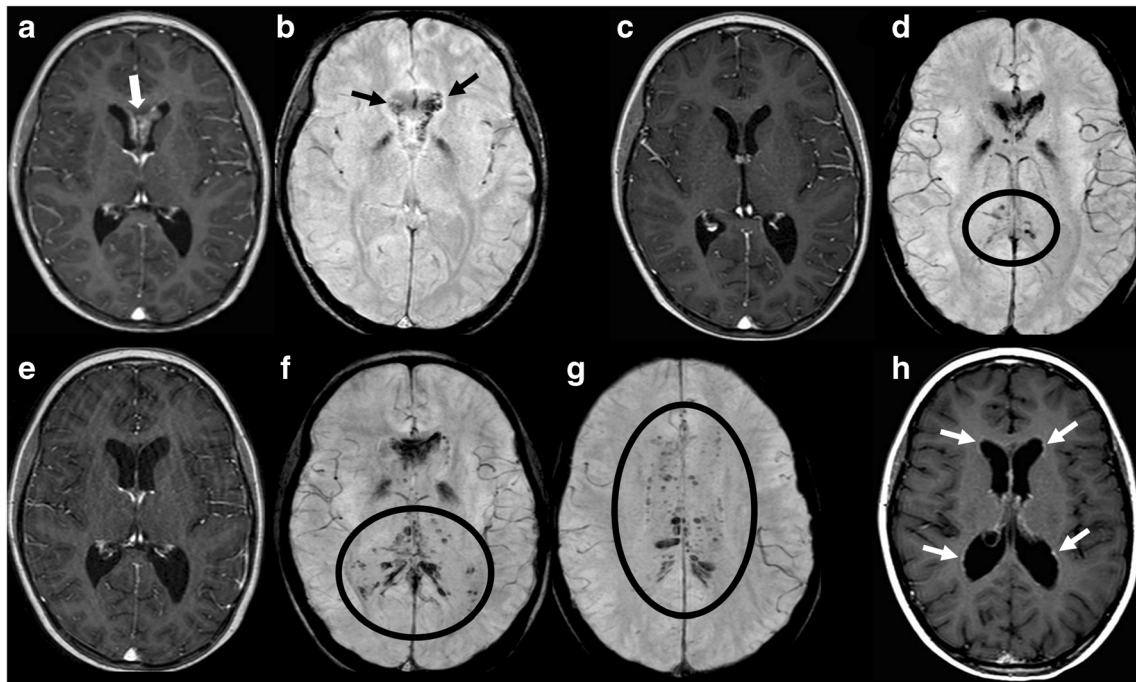


Fig. 5 Recurrent disease in a 10-year-old girl with NGGCT (same patient as in Fig. 4). **a, b** Follow-up MRI 10 months after the end of treatment. Gadolinium-enhanced axial T1-weighted image shows pathologic tissue with contrast enhancement along the frontal horns in keeping with relapse (thick white arrow, **a**). Axial SWI image demonstrates hypointense foci along the frontal horns (thin black arrows, **b**). There is persistence of the hypointense foci within the bilateral globus pallidus. **c, d** Follow-up MRI 2 months after re-treatment (radiotherapy). Gadolinium-enhanced axial T1-weighted image demonstrates complete resolution of the pathologic contrast enhancement (**c**). Axial SWI image shows persistence of hypointense

foci along the frontal horns and globus pallidus, bilaterally (**d**) and evidence of tiny hypointense foci, not present in the prior examination, along the posterior wall of the lateral ventricles (black circle, **d**). **e–g** Follow-up MRI 4 months after re-treatment. Gadolinium-enhanced axial T1-weighted image does not show residual/recurrent disease (**e**); however, axial SWI images demonstrate worsening of hypointense foci along the wall of the lateral ventricles (black circle, **f, g**). **h** Follow-up MRI 8 months after re-treatment. Gadolinium-enhanced axial T1-weighted image now shows tiny nodules of contrast enhancement along the walls of the lateral ventricles (thin white arrow, **h**)

main lesion in two patients with NGGCT and marked SWI hypointensity of the primary lesion. In one subject, hypointense foci corresponded to foci of dissemination on conventional pre- and post-contrast T1-/T2-weighted imaging (Fig. 4); on follow-up, this patient presented disease relapses, again characterized by the presence of hypointense foci on SWI (Fig. 5 and supplementary Figure S1).

In another patient, there were no corresponding abnormalities on standard imaging. In this subject, despite negative CSF cytology and lack of signs of secondary dissemination on conventional brain and spine MRI, craniospinal irradiation was performed on the basis of SWI findings which raised the suspicion of secondary dissemination. Follow-up MRI demonstrated reduction of SWI hypointensities following treatment (Fig. 3). To the best of our knowledge, these findings have never been reported and, paralleling the role of SWI for basal ganglia involvement recognition, might suggest a potential role of this sequence in the detection of secondary dissemination from NGGCT presenting with extensive microbleeds of the primary lesion. In subjects with metastatic pure germinomas, secondary lesions detected on conventional

imaging did not show hypointensity on SWI/GRE, similarly to primary lesions. Even this finding might be helpful for differentiating pure germinomas from NGGCT.

Of note, brain hypointense foci on T2*-based MR imaging are a common secondary effect of radiotherapy treatment in children, likely corresponding to microbleeds, capillary telangiectasias, and/or small cavernomas [31–33]. Typically, these lesions do not show contrast enhancement. However, in patients with NGGCT and marked SWI hypointensity of the primary lesion at presentation, the appearance of new SWI hypointensities on follow-up in areas of typical disease relapse, such as the subependymal region, should alert clinicians, because even though radiation-induced lesions are common, foci of disease relapse cannot be excluded.

Given the limited number of patients with dissemination or disease relapse evaluated in this study, larger series are necessary to better understand the potential role of SWI/GRE imaging in this field.

T2*-based MR imaging was available on follow-up in four out of five patients with basal ganglia involvement demonstrating persistence of hypointensity within the basal ganglia

in one patient and reduction in three subjects. Persistence of basal ganglia T2* hypointensity on follow-up remains unclear and might be related to persistence of hemosiderin or iron deposition rather than active disease. Larger studies are needed to elucidate the pathomechanism of such changes in basal ganglia.

Our results should be interpreted with awareness of some limitations. A limited number of patients were studied; however, we included only children with intracranial GCT undergoing T2*-based MR imaging, which is not a commonly used MR sequence in the evaluation of these rare tumors. Another limitation concerns the selection of patients included in retrospective analyses. Because not all pediatric patients with intracranial GCT underwent T2*-based MR imaging, selection bias may have played a role in the interpretation of data, and the distribution of lesions may not be entirely reflective of the epidemiology of intracranial GCT. We also recognize that histological verification of secreting lesions was not performed; therefore, a precise radiological and histological correlation was not possible. However, current standards in Europe and North America do not require histological confirmation for secreting intracranial GCT diagnosis.

In conclusion, assessment of the SWI or T2* GRE characteristics of intracranial GCT may assist in differentiating pure germinomas from NGGCTs and can provide additional clues in the identification and characterization of basal ganglia germinomas. Further investigations on larger series are awaited to elucidate the role of SWI in assessing dissemination in NGGCT.

Compliance with ethical standards

Funding No funding was received for this study.

Conflict of interest The authors declare that they have no conflict of interest.

Ethical approval All procedures performed in studies involving human participants were in accordance with the ethical standards of the institutional and/or national research committee and with the 1964 Helsinki declaration and its later amendments or comparable ethical standards.

For this type of study formal consent is not required.

Informed consent For this type of retrospective study formal consent is not required; however, informed consent was obtained from all individual participants included in the study or their legal guardians, and patient assent was obtained whenever appropriate.

References

- Packer RJ, Cohen BH, Cooney K (2000) Intracranial germ cell tumors. *Oncologist* 5:312–320
- Weiner HL, Finlay JL (1999) Surgery in the management of primary intracranial germ cell tumors. *Childs Nerv Syst* 15:770–773
- Ogiwara H, Tsutsumi Y, Matsuoka K, Kiyotani C, Terashima K, Morota N (2015) Apparent diffusion coefficient of intracranial germ cell tumors. *J Neuro-Oncol* 121:565–571
- Goldman S, Bouffet E, Fisher PG, Allen JC, Robertson PL, Chuba PJ et al (2015) Phase II trial assessing the ability of neoadjuvant chemotherapy with or without second-look surgery to eliminate measurable disease for nongerminomatous germ cell tumors: a Children's Oncology Group Study. *J Clin Oncol* 33:2464–2471
- Echevarría ME, Fangusaro J, Goldman S (2008) Pediatric central nervous system germ cell tumors: a review. *Oncologist* 13:690–699
- Phi JH, Cho BK, Kim SK, Paeng JC, Kim IO, Kim IH et al (2010) Germinomas in the basal ganglia: magnetic resonance imaging classification and the prognosis. *J Neuro-Oncol* 99:227–236
- Lee SM, Kim IO, Choi YH, Cheon JE, Kim WS, Cho HH, You SK (2016) Early imaging findings in germ cell tumors arising from the basal ganglia. *Pediatr Radiol* 46:719–726
- Minami N, Tanaka K, Kimura H, Hirose T, Mori T, Maeyama M et al (2016) Radiographic occult cerebellar germinoma presenting with progressive ataxia and cranial nerve palsy. *BMC Neurol* 16:4
- Loto MG, Danilowicz K, González Abbati S, Torino R, Misiunas A (2014) Germinoma with involvement of midline and off-midline intracranial structures. *Case Rep Endocrinol* 2014:936937
- Murray MJ, Bartels U, Nishikawa R, Fangusaro J, Matsutani M, Nicholson JC (2015) Consensus on the management of intracranial germ-cell tumours. *Lancet Oncol* 16:e470–e477
- Calaminus G, Kortmann R, Worch J, Nicholson JC, Alapetite C, Garrè ML et al (2013) SIOP CNS GCT 96: final report of outcome of a prospective, multinational nonrandomized trial for children and adults with intracranial germinoma, comparing craniospinal irradiation alone with chemotherapy followed by focal primary site irradiation for patients with localized disease. *Neuro-Oncology* 15:788–796
- Morana G, Maghnie M, Rossi A (2010) Pituitary tumors: advances in neuroimaging. *Endocr Dev* 17:160–174
- Chavhan GB, Babyn PS, Thomas B, Shroff MM, Haacke EM (2009) Principles, techniques, and applications of T2*-based MR imaging and its special applications. *Radiographics* 29:1433–1449
- Tong KA, Ashwal S, Obenaus A, Nickerson JP, Kido D, Haacke EM (2008) Susceptibility-weighted MR imaging: a review of clinical applications in children. *AJNR Am J Neuroradiol* 29:9–17
- Lou X, Ma L, Wang FL, Tang ZP, Huang H, Cai YQ, Wong EH (2009) Susceptibility-weighted imaging in the diagnosis of early basal ganglia germinoma. *AJNR Am J Neuroradiol* 30:1694–1699
- Fujii Y, Saito Y, Ogawa T, Fujii S, Kamitani H, Kondo S et al (2008) Basal ganglia germinoma: diagnostic value of MR spectroscopy and (11)C-methionine positron emission tomography. *J Neurol Sci* 270:189–193
- Wang Y, Zou L, Gao B (2010) Intracranial germinoma: clinical and MRI findings in 56 patients. *Childs Nerv Syst* 26:1773–1777
- Sumida M, Uozumi T, Kiya K, Mukada K, Arita K, Kurisu K et al (1995) MRI of intracranial germ cell tumours. *Neuroradiology* 37:32–37
- Liang L, Korogi Y, Sugahara T, Ikushima I, Shigematsu Y, Okuda T et al (2002) MRI of intracranial germ-cell tumours. *Neuroradiology* 44:382–388
- Fujimaki T, Matsutani M, Funada N, Kirino T, Takakura K, Nakamura O et al (1994) CT and MRI features of intracranial germ cell tumors. *J Neuro-Oncol* 19:217–226
- Awa R, Campos F, Arita K, Sugiyama K, Tominaga A, Kurisu K et al (2014) Neuroimaging diagnosis of pineal region tumors—quest for pathognomonic finding of germinoma. *Neuroradiology* 56:525–534
- Mufti ST, Jamal A (2012) Primary intracranial germ cell tumors. *Asian J Neurosurg* 7:197–202
- Woo PYM, Chu ACH, Chan KY, Kwok JCK (2017) Progressive hemiparesis in a young man: hemispheric atrophy as the initial

- manifestation of basal ganglia germinoma. *Asian J Neurosur* 12: 65–68
24. Perry BC, Perez FA, Nixon JN, Cole BL, Ishak G (2017) Primary choriocarcinoma of the bilateral basal ganglia presenting in a teen-aged male. *Radiol Case Rep* 12:154–158
 25. Sartori S, Laverda AM, Calderone M, Carollo C, Viscardi E, Faggin R, Perilongo G (2007) Germinoma with synchronous involvement of midline and off-midline structures associated with progressive hemiparesis and hemiatrophy in a young adult. *Childs Nerv Syst* 23:1341–1345
 26. Di Iorgi N, Morana G, Napoli F, Allegri AE, Rossi A, Maghnie M (2015) Management of diabetes insipidus and adipsia in the child. *Best Pract Res Clin Endocrinol Metab* 29:415–436
 27. Oyama N, Terae S, Saitoh S, Sudoh A, Sawamura Y, Miyasaka K (2005) Bilateral germinoma involving the basal ganglia and cerebral white matter. *ANJR Am J Neuroradiol* 26:1166–1169
 28. Kim DI, Yoon PH, Ryu YH, Jeon P, Hwang GJ (1998) MRI of germinomas arising from the basal ganglia and thalamus. *Neuroradiology* 40:507–511
 29. Bekiesinska-Figatowska M, Mierzevska H, Jurkiewicz E (2013) Basal ganglia lesions in children and adults. *Eur J Radiol* 82:837–849
 30. Rossi A, Garrè ML, Ravegnani M, Nozza P, Abbruzzese A, Giangaspero F, Tortori-Donati P (2008) Bilateral germinoma of the basal ganglia. *Pediatr Blood Cancer* 50:177–179
 31. Peters S, Pahl R, Claviez A, Jansen O (2013) Detection of irreversible changes in susceptibility-weighted images after whole-brain irradiation of children. *Neuroradiology* 55:853–859
 32. Di Giannatale A, Morana G, Rossi A, Cama A, Bertoluzzo L, Barra S et al (2014) Natural history of cavernous malformations in children with brain tumors treated with radiotherapy and chemotherapy. *J Neuro-Oncol* 117:311–320
 33. Varon D, Simons M, Chiang F, Tedeschi G, Pacheco G, Martinez P, Castillo M (2014) Brain radiation-related black dots on susceptibility-weighted imaging. *Neuroradiol J* 27:445–451